BRAF V600E in a preclinical model of pleomorphic Xanthoastrocytoma: Analysis of the tumor microenvironment and immune cell infiltration dynamics *in vivo*

Alessandro Canella,[1] Matthew Nazzaro,[1] Mykyta Artomov,[1,2] Lakshmi Prakruthi Rao Venkata,[1] Diana Thomas,[3] Justin Lyberger,[4] Aleksandr Ukhatov,[5] Yao Lulu Xing,[6] Katherine Miller,[1] Gregory Behbehani,[4,7] Nduka M. Amankulor,[8] Claudia Katharina Petritsch,[6] and Prajwal Rajappa[1,2,9]

[1]The Steve and Cindy Rasmussen Institute for Genomic Medicine, Nationwide Children's Hospital, Columbus, OH, USA; [2]Department of Pediatrics, The Ohio State University Wexner Medical Center, Columbus, OH, USA; [3]Department of Pathology and Laboratory Medicine, Nationwide Children's Hospital, Columbus, OH, USA; [4]Department of Medicine, Division of Hematology, The Ohio State University Comprehensive Cancer Center, The Ohio State University, Columbus, OH, USA; [5]Department of Electrical Engineering. Korea Advanced Institute of Science and Technology, Daejeon, Republic of Korea; [6]Department of Neurosurgery, Stanford University School of Medicine, Stanford, CA, USA; [7]Pelotonia Institute for Immuno-Oncology, The Ohio State University, Columbus, OH, USA; [8]Department of Neurosurgery, University of Pennsylvania, Philadelphia, PA, USA; [9]Department of Neurological Surgery, The Ohio State University Wexner Medical Center, Columbus, OH, USA

Low-grade glioma (LGG) is the most common brain tumor affecting pediatric patients (pLGG) and BRAF mutations constitute the most frequent genetic alterations. Within the spectrum of pLGGs, approximately 70%–80% of pediatric patients diagnosed with transforming pleomorphic xanthoastrocytoma (PXA) harbor the BRAF V600E mutation. However, the impact of glioma BRAF V600E cell regulation of tumor-infiltrating immune cells and their contribution to tumor progression remains unclear. Moreover, the efficacy of BRAF inhibitors in treating pLGGs is limited compared with their impact on BRAF-mutated melanoma. Here we report a novel immunocompetent RCAS-BRAF V600E murine glioma model. Pathological assessment indicates this model seems to be consistent with diffuse gliomas and morphological features of PXA. Our investigations revealed distinct immune cell signatures associated with increased trafficking and activation within the tumor microenvironment (TME). Intriguingly, immune system activation within the TME also generated a pronounced inflammatory response associated with dysfunctional CD8+ T cells, increased presence of immunosuppressive myeloid cells and regulatory T cells. Further, our data suggests tumor-induced inflammatory processes, such as cytokine storm. These findings suggest a complex interplay between tumor progression and the robust inflammatory response within the TME in preclinical BRAF V600E LGGs, which may significantly influence animal survival.

INTRODUCTION

Pediatric low-grade glioma (pLGG) is the most prevalent brain tumor in children.[1] Most pLGGs are characterized by indolent growth and a diverse array of heterogeneity and histological subtypes, thus posing unique clinical challenges in terms of diagnosis, prognosis, and therapeutic management. Although overall survival in pLGG is considered relatively favorable compared with other brain tumors, several factors, including tumor location, partial surgical resection, limitation of radiation therapy in young patients, chemoresistance to conventional therapies, resistance to BRAF inhibitors in BRAF-mutated patients, and occurrence of neurofibromatosis type 1 (NF1) mutations, significantly affect long-term survival rates.[2–7]

Previously classified based on histological features, pLGG is now stratified into molecular subgroups. The molecular landscape of pLGG was recently delineated with the identification of key genetic alterations, and the BRAF V600E mutation recently emerged as a pivotal driver in tumor progression, presenting new opportunities for research, diagnosis, and targeted therapies. Its incidence varies in pLGG patients, ranging from 3% in cases of pilocytic astrocytoma to up to 80% in transforming pleomorphic xanthoastrocytoma (PXA).[6,8,9] PXA pediatric patients with BRAF V600E mutation have tumor of World Health Organization grade II and III, with a 3- to 5-year progression-free survival of over 60%.[10] While
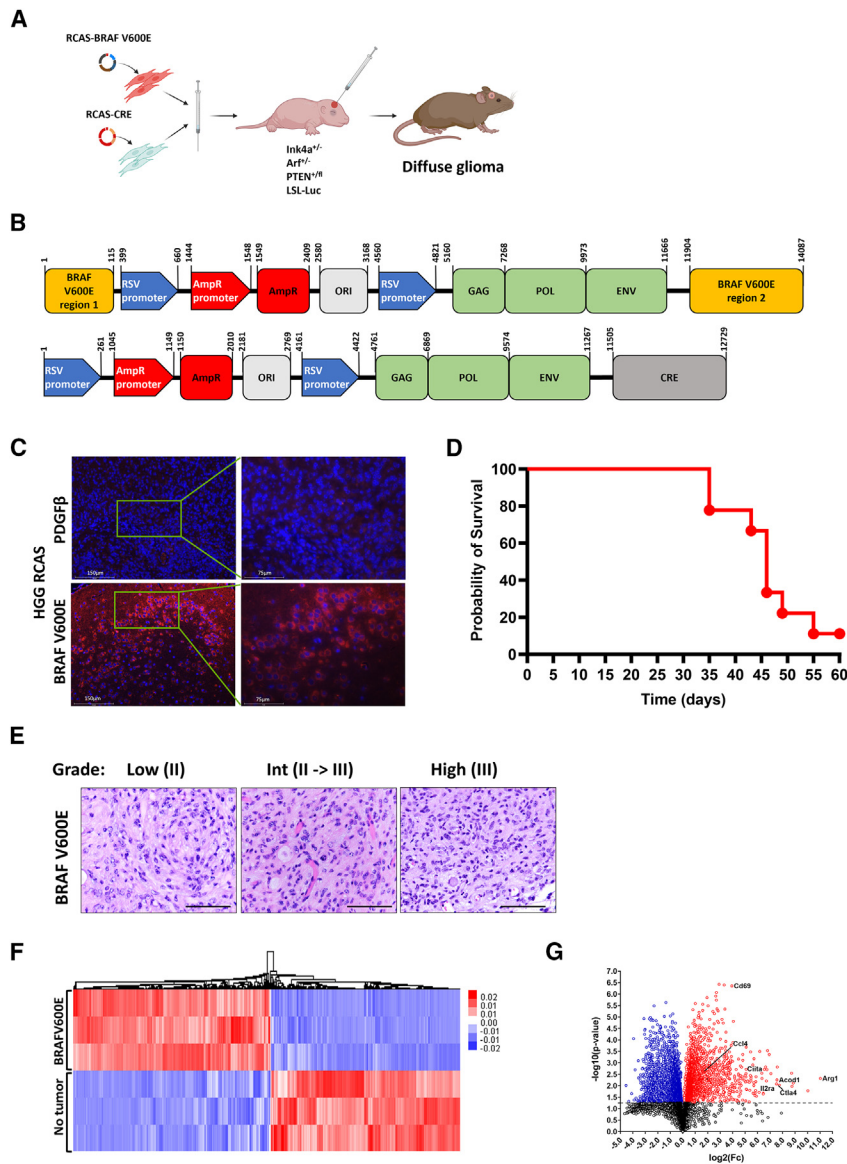
Figure 1. Establishment of the immunocompetent RCAS-BRAF V600E murine model

(A) Schematic of the induction of gliomagenesis in RCAS-BRAF V600E model (biorender.com). (B) Representation of the RCAS-BRAF V600E and RCAS-CRE linearized plasmids. (C) Immune fluorescence of coronal brain sections of RCAS-PDGFβ (above, BRAF V600E negative, $n = 3$) and RCAS-BRAF V600E (below, $n = 4$) mice at the endpoints, for the evaluation of BRAF V600E (red) and nuclei (Hoechst, blue). Left panels have been acquired with $20\times$ magnification, right panels with $40\times$ magnification. (D) Survival study of RCAS-BRAF V600E animals evaluated by Kaplan-Meier curves. Mice were injected with 50,000 DF1-RCAS-BRAF V600E and 50,000 DF1-RCAS-CRE cells in the right hemisphere bregma of pups at days 0–2 of age ($n = 9$). Median survival was calculated at day 46 after induction of gliomagenesis. (E) Hematoxylin and eosin-stained images of 5 μm paraffin-embedded coronal brain sections isolated from of RCAS-BRAF V600E animals #2, #3, and #5 at the endpoints (Table S2; scale bar, 100 μm). (F) Dendrogram of the unsupervised hierarchical clustering analysis of total RNA-seq in intratumoral immune cells ($n = 3$) from RCAS-BRAF V600E animals compared with no tumor animals ($n = 3$). (G) Volcano plot of the differential gene expression of tumor-infiltrating immune cells. In total, 8,085 genes. In red are the genes significantly upregulated, and in blue are the genes significantly downregulated. Unpaired two-tailed Student's t test calculated statistical significance.

glioma cells,[15] underscoring the necessity for a deeper comprehension of tumor biology and mechanisms of tumor progression enhanced by the tumor microenvironment (TME). Recent glioma studies pointed out the crucial role of the immunosuppressive TME, primarily orchestrated by myeloid and regulatory T cells (Tregs),[16–20] in disease progression. However, the investigation of tumor-infiltrating immune cells *in vivo* in BRAF-mutated pLGG remains largely unexplored. In this study, we used a novel RCAS-BRAF V600E immunocompetent murine model to characterize the tumor-infiltrating immune cells during later stages of tumor progression.

RESULTS

The novel RCAS immunocompetent animal model resembles PXA LGG characteristics

To initiate gliomagenesis in the right cerebral hemisphere of transgenic NTV-a; Ink4a$^{+/-}$Arf$^{+/-}$;PTEN$^{+/fl}$; LSL-Luc mice, chicken fibroblasts (DF1 cells) engineered for the release of RCAS-BRAF V600E and RCAS-CRE retroviruses were injected. Gliomagenesis occurred due to the combined effect of ectopic BRAF V600E expression and loss of floxed PTEN by CRE (Figures 1A–1C). The animals monitored in the survival study revealed a decline starting at the end of the fifth week after induction of

surgical resection can be curative in a subset of patients, a notable portion of pLGG patients with BRAF V600E mutation experience tumor transformation to pediatric high-grade glioma (HGG), tumor relapse, rapid progression, and propagation through the brain.[10,11] The valine to glutamine missense mutation results in constitutive activation of the mitogen-activated protein kinase (MAPK) pathway, a crucial signaling cascade driving cancer cellular proliferation and survival.[12] When coupled with the loss of function of CDKN2A, a cell cycle regulator and onco-suppressor, the BRAF V600E mutation was associated with pLGG malignant transformation[11,13] and recapitulated in murine models.[14] Consistent with the efficacy of BRAF inhibition (BRAFi) against melanoma and lung cancer, the use of type 1 BRAFi in treating BRAF-mutated pLGG has shown increased MAPK activation in
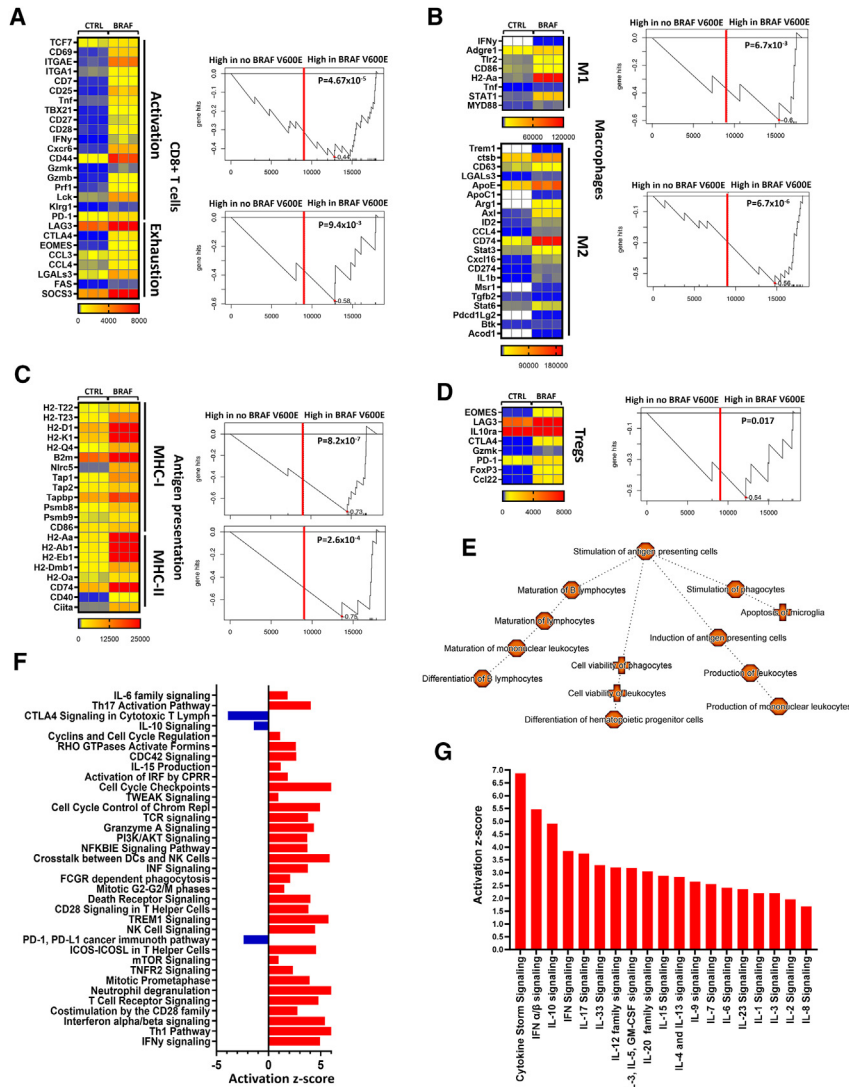
Figure 2. The transcriptome from tumor-infiltrating immune cells in RCAS-BRAF V600E animals at the late stage of the tumor progression and comparison with human pLGG

Tumor-infiltrating immune cells were harvested at day 50 post-induction of gliomagenesis and analyzed by total RNA-seq in comparison with corresponding RNA samples from no tumor animals ($n = 3$). (A–D) Heatmaps were generated using significant and differentially expressed genes associated with (A) CD8$^+$ cytotoxic T cells, (B) Tregs, (C) antigen presentation, and (D) macrophages. The plots on the right side of (A–D) show the differential gene enrichment of corresponding gene expression signatures among genes upregulated in human BRAF V600E LGGs. Kolmogorov-Smirnov was used to calculate statistical significance. (E) Graphical summary of the gene enrichment analysis performed by ingenuity pathway analysis (IPA). (F) Top 35 canonical pathways differentially and significantly expressed by tumor-infiltrating immune cells isolated from RCAS-BRAF V600E or control animals. (G) IPA prediction of the significant upregulation of cytokine storm signaling pathway and of several cytokine signaling pathways in tumor immune cells. Unpaired two-tailed Student's t test calculated statistical significance.
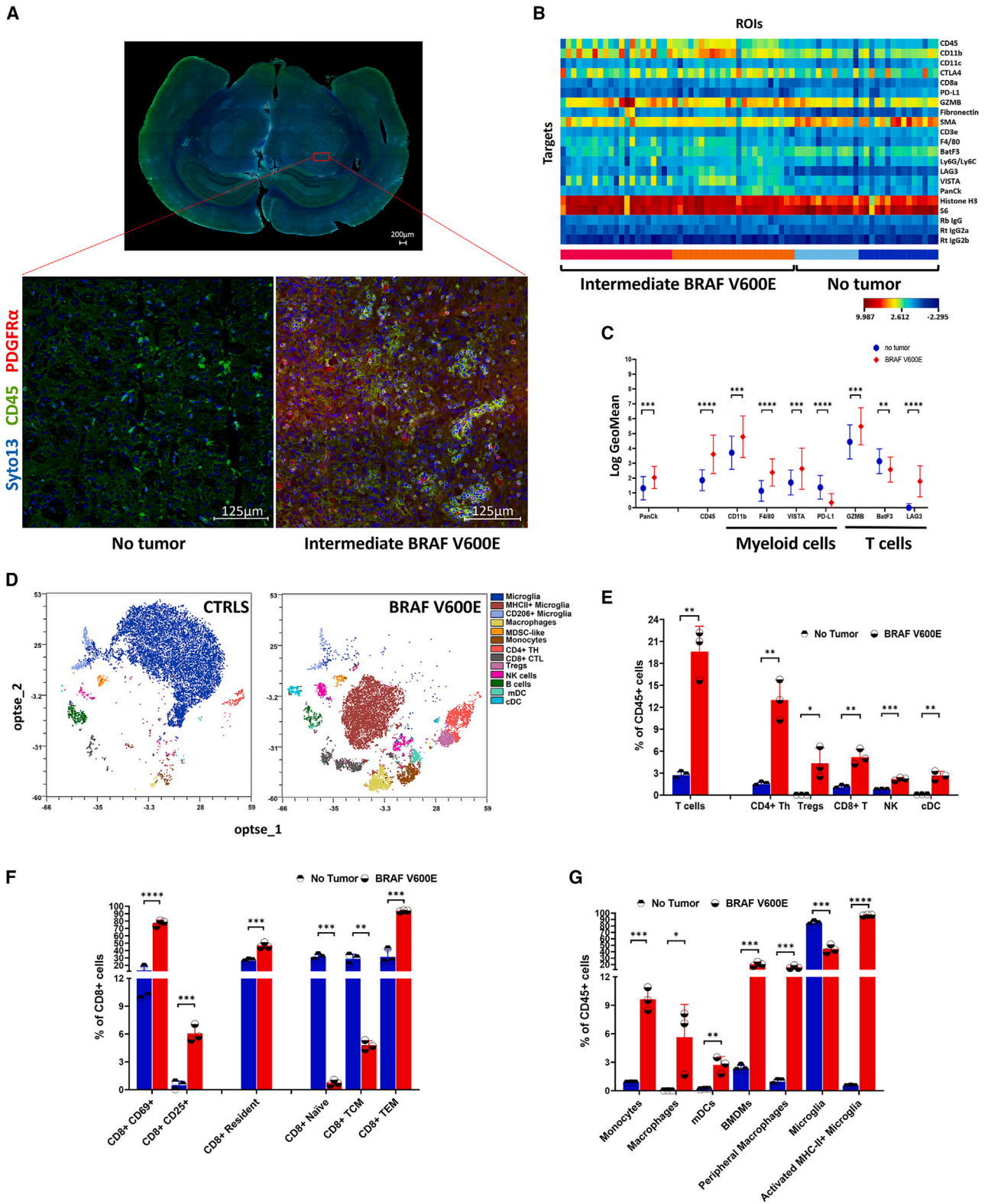
immunocompetent PXA pLGG animal model described in the literature. Although the tumor morphology, progression, and survival in BRAF V600E PXA patients have been already described in literature, the evaluation of the immune TME within this disease entity has not been studied extensively.

Infiltration, overstimulation, and exhaustion: Decoding immune cell transcriptomes in the BRAF V600E glioma microenvironment *in vivo*

Total RNA sequencing (RNA-seq) was performed of tumor-infiltrating immune cells iso-

gliomagenesis, with a median survival of 46 days (Figure 1D). Neuropathological evaluation of hematoxylin and eosin-stained brain sections from animals at endpoints revealed that six out of seven developed diffuse gliomas (Figure 1E; Table S2). Based on cancer cell morphology, tumor infiltration, cells in mitosis, microvascular proliferation, and absent necrosis, one animal was classified as LGG, whereas three were transitioning from LGG to HGG, and three had HGG. During the survival study, an asymptomatic animal euthanized on day 60 revealed intermediate LGG to HGG neoplastic cell infiltration in both brain hemispheres (Figure 1E). Therefore, tumor infiltration, the presence of mitotic bodies, rare microvascular proliferation, and absent necrosis led us to classify the tumor as a transforming diffuse glioma (Figure 1E; Table S2). Notably, these neoplastic cells presented morphological features similar to the PXA in pLGG, including multivacuolated cytoplasm, rare microvascular proliferation, and absence of necrosis.[10] This animal model, to our knowledge, represents the first

lated from the TME of RCAS-BRAF V600E animals at day 50 post-induction of gliomagenesis, near endpoints. As a negative control, we isolated immune cells from the right hemisphere of no tumor animals sharing the same genetic background and age. RNA-seq identified 8,085 genes that exhibited significant differential expression in RCAS-BRAF V600E animals compared with control animals (Figures 1F and 1G). Among these genes, 4,127 genes were upregulated, while 3,959 were downregulated (GEO: GSE252367) (Table S4). Genes associated with myeloid cell immunosuppression (Arg1, Fc = 2,080.2) and cytotoxic T cell exhaustion (CTLA4, Fc = 182.15) were among the top differentially expressed (Figure 1G). While our previous studies demonstrated a robust immunosuppressive TME supporting tumor progression in the RCAS-PDGFβ glioma murine model,[19] the RNA-seq signature in BRAF V600E mice showed upregulation of genes associated with CD8$^+$ T cell activation and exhaustion (Figure 2A), proinflammatory (M1) and immunosuppressive (M2)

myeloid cells (Figure 2B), antigen presentation (Figure 2C), as well as Treg activation (Figure 2D). To corroborate our findings *in vivo* with pediatric BRAF V600E gliomas, we assessed the similarity between the characteristic gene expression signatures observed in the mouse model and those present in the human tumors. Differential gene expression analysis was performed for nine pLGGs with BRAF V600E and a control group consisting of 80 tumors lacking this somatic mutation. We have observed consistent and significant upregulation of CD8$^+$, M1/M2 macrophage, antigen presentation, and Treg signatures in the human BRAF V600E tumors (Figures 2A–2D, right, and S4A), aligning with observations in the mouse model.

In addition, a gene enrichment analysis using ingenuity pathway analysis confirmed immune cell infiltration and proliferation (Figure 2E). The top 35 canonical signaling pathways revealed activation of CD4$^+$ T, CD8$^+$ T, and NK cells (Figures 2F; S1). Interestingly, it also predicted the upregulation of 18 distinct cytokine signaling pathways as well as signaling associated with cytokine storm (Figures 2G; S2). Moreover, the analysis of pathological pathways highlighted the upregulation of the hypersensitivity reaction and of the hemophagocytic lymphohistiocytosis pathways. These pathways are linked with an overstimulated immune system, and uncontrolled activation of CD8+ T cells (Figure S3).[21] Based on these results, we suggest that the phenotypic decline of the BRAF V600E animals might be attributed to a combinatorial effect of tumor progression combined with an aberrant inflammatory immune cascade within the TME.

Immune cell response within the BRAF V600E glioma microenvironment *in vivo*

To corroborate our RNA-seq findings, we utilized GeoMX digital spatial transcriptomic profiling (DSP, Figures 3A–3C; S4B–S4D), and mass cytometry (CyTOF, Figures 3D–3G). To investigate the tumor immune cell infiltration, we stained brain sections of intermediate glioma BRAF-mutated mice at the endpoints and control mice with PDGFRα (cancer cell marker), CD45 (pan-immune cell marker), and Syto13 (nuclear marker, Figure 3A). In addition, the tissues were also hybridized with specific GeoMX modules for cell typing and profiling (Supplemental Methods).

As expected, DSP acquisition and analysis of different regions of interest (ROIs, 44 for BRAF V600E and 27 for no tumor controls),

showed the significant upregulation of markers associated with cancer cells (PanCK) and immune cells (CD45). Increased infiltration of macrophages (CD11b, F4/80) and markers associated with CD8+ T cell activation (Gzmb) or exhaustion (Lag3) were evident in the glioma TME, as compared with controls (Figures 3B and 3C). Moreover, we isolated immune cells from BRAF V600E animals at day 50 and analyzed the phenotype by CyTOF (Figures 3D–3G; Table S3). The t-Distributed Stochastic Neighbor Embedding (t-SNE) maps in Figure 3D showed a population of significantly activated microglia in BRAF mutated animals accompanied by an infiltration of proinflammatory macrophages and monocytes, immunosuppressive myeloid-derived suppressor cells (MDSC), T lymphocytes, dendritic cells (DC), and natural killer (NK) cells (Figures 3E–3G). These results clearly demonstrate a profuse inflammation in the TME. Among T lymphocytes, increased infiltration of CD8$^+$ cytotoxic, CD4$^+$ T helper cells (Th), and Tregs was observed in the BRAF V600E TME (Figure 3E). While CyTOF analysis highlighted the activation status of CD8$^+$ T cells (Figure 3F; Table S3), it was not possible to assess the exhaustion status of T cells due to lack of specific markers in the panel such as Lag3, Tim-3, and TOX. In summary, our analysis of the immune cellular phenotype in the glioma BRAF V600E TME highlights a distinct profile of immune cell infiltration during the late stage of the tumor progression. Specifically, our findings reveal a unique pattern characterized by the infiltration of activated cytotoxic T cells and NK cells, alongside both pro-inflammatory and immunosuppressive myeloid cells. Notably, this differs from previous reports on RCAS IDH1 R132H and IDH1 wild-type glioma models.[19,22]

DISCUSSION

BRAF mutations represent the prevalent genetic alteration in pediatric glioma patients. Clinical evaluation of BRAF inhibitors for treating BRAF-mutated pLGG showed toxicity and acquired resistance to these treatments.[4,7,15,23] Moreover, there is a paucity of immunocompetent BRAF-mutated glioma murine models for the scientific community to elucidate these mechanisms of resistance.[24] Here, we present a novel immunocompetent RCAS-BRAF V600E murine model that resembles diffuse glioma PXA pLGG-like tumors. These tumors spontaneously transform from grade II to III until the mice decline. In addition, our study describes the characteristics of the tumor-infiltrating immune cells after transformation *in vivo*. Upon harvesting the immune cells from the TME of RCAS-BRAF V600E mice, our findings indicate

Figure 3. Analysis of the phenotype of tumor-infiltrating immune cells in RCAS-BRAF V600E animals

(A–C) Brains from glioma animals (at the endpoints, samples #1 and #3 of Figure 1E) or from control animals were processed for GeoMX DSP. (A) Coronal sections were deparaffinated and stained for Syto13 (nuclei), CD45-AF594 (immune cells), PDGFRα-AF647 (cancer cells), mouse immune cell typing module (Nanostring), mouse immune cells profiling core (Nanostring), and mouse immuno-oncology drug target module (Nanostring) (*n* = 3). (B) A total of 44 regions of interest (ROIs) from BRAF V600E slides (*n* = 2) and 17 from no tumor control slides (*n* = 2) were isolated for spatial profiling. After data normalization, the heatmap was created with the significant and differential expressed targets. Housekeeping targets (S6 and histone H3) and background targets (Rb IgG, Rt IgG2a, and Rt IgG2b) were used for the data normalization. (C) Expression levels of the most relevant and significant DSP targets, calculated as log geomean average/ROI. (D–G) Tumor-infiltrating immune cells were harvested at day 50 after induction of gliomagenesis and analyzed by mass cytometry compared with samples from no tumor animals (*n* = 3). (D) t-Distributed stochastic neighbor embedding map of the tumor-infiltrating immune cells in no tumor control (CTRLS) and BRAF V600E animals. (E) Characterization of the tumor-infiltrating CD45$^+$, (F) CD8$^+$ T, and G) myeloid cells. Unpaired two-tailed Student's *t* test calculated statistical significance.

that immune cell infiltration is characterized by both activated and exhausted cytotoxic CD8^{+} T cells, CD4^{+} Th, and Tregs, as well as proinflammatory and immunosuppressive myeloid cells. These findings are in line with earlier study demonstrating the presence of these T cell populations in a syngeneic murine model for BRAF V600E HGGs.[25] Moreover, the prominent inflammatory response within the TME seems to have caused signatures associated with cytokine storm, hypersensitivity, and hemophagocytic lymphohistiocytosis. Therefore, in addition to treatment response, this model can be particularly useful for investigating the mechanisms of immune escape employed by BRAF-mutated glioma cells to evade immune surveillance. In addition, the model could be beneficial for translational projects aiming to evaluate novel BRAF inhibitors or to modulate inflammation and immunosuppression in gliomas. This model will also allow for a greater appreciation of the fundamental biology of cytokine associated toxicities and how to modulate an overstimulated immune response. While the mechanisms of immune escape adopted by glioma cells during tumor progression remain unclear, future studies using this model will be necessary to evaluate and quantify the immune cell infiltration at earlier stages of tumor progression and at the endpoints, to study the mechanisms of tumor immune evasion, and to test the therapeutic effect of BRAF inhibitors in BRAF V600E models *in vivo*.

MATERIALS AND METHODS
Additional methods are detailed in the Supplemental material.[19,20,26,27]

Mouse model
Gliomagenesis *in vivo* was induced in NTV-a; Ink4a^{+/−} Arf^{+/−};PTEN^{+/fl};LSL-Luc model, using RCAS system as previously described.[19,28–30] Pups at 0 to 2 days of age were injected with 1 μL DPBS (Gibco) containing the DF1-BRAF V600E ([Figure 1]B) and DF1-CRE[30] cell lines (50,000 cells/kind) ([Figure 1]A). The RCAS retrovirus particles released into the right hemisphere in brain of pups at the age of 0–2 days targeted and induced transduction of neural stem cells expressing the T-va receptor. Negative control animals without tumors shared the same genetic profile and age. Animal studies were approved by Nationwide Children's Hospital Institutional Animal Care and Use Committee (protocol # AR19-00146).

Quantification and statistical analysis
The results were generated by at least three independent observations. Overall survival was measured by Kaplan-Meier curve. To assess the statistical significance ($p < 0.05$), survival analyses (Mantel-Cox) and unpaired two-tailed Student's *t* test were calculated using GraphPad (Prism). Statistical significance was indicated as *$p < 0.05$, **$p < 0.01$, ***$p < 0.001$, and ****$p < 0.0001$.

DATA AND CODE AVAILABILITY
Upon request, the corresponding authors will grant access to all data for the scientific community.

AUTHOR CONTRIBUTIONS
P.R. and C.K.P conceptualized the project. A.C. developed the project and designed the experiments. A.C., L.P.R.V., and J.L. performed experiments; A.C., M.N., and D.T. interpreted the data; M.A. and A.U. analyzed the human data; Y.L.X. and C.K.P. provided the RCAS-BRAF V600E plasmid; A.C. wrote the manuscript. All authors were involved in the final editing. P.R. approved the final manuscript.

DECLARATION OF INTERESTS
P.R. is an associate editor of Molecular Therapy Oncology.

REFERENCES
1. Ostrom, Q.T., Price, M., Neff, C., Cioffi, G., Waite, K.A., Kruchko, C., and Barnholtz-Sloan, J.S. (2022). CBTRUS Statistical Report: Primary Brain and Other Central Nervous System Tumors Diagnosed in the United States in 2015-2019. Neuro. Oncol. *24*, v1–v95. https://doi.org/10.1093/neuonc/noac202.

2. Armstrong, G.T., Conklin, H.M., Huang, S., Srivastava, D., Sanford, R., Ellison, D.W., Merchant, T.E., Hudson, M.M., Hoehn, M.E., Robison, L.L., et al. (2011). Survival and long-term health and cognitive outcomes after low-grade glioma. Neuro. Oncol. *13*, 223–234. https://doi.org/10.1093/neuonc/noq178.

3. Bandopadhayay, P., Bergthold, G., London, W.B., Goumnerova, L.C., Morales La Madrid, A., Marcus, K.J., Guo, D., Ullrich, N.J., Robison, N.J., Chi, S.N., et al. (2014). Long-term outcome of 4,040 children diagnosed with pediatric low-grade gliomas: an analysis of the Surveillance Epidemiology and End Results (SEER) database. Pediatr. Blood Cancer *61*, 1173–1179. https://doi.org/10.1002/pbc.24958.

4. Capogiri, M., De Micheli, A.J., Lassaletta, A., Muñoz, D.P., Coppé, J.-P., Mueller, S., and Guerreiro Stucklin, A.S. (2022). Response and resistance to BRAFV600E inhibition in gliomas: Roadblocks ahead? Front. Oncol. *12*, 1074726. https://doi.org/10.3389/fonc.2022.1074726.

5. Manoharan, N., Liu, K.X., Mueller, S., Haas-Kogan, D.A., and Bandopadhayay, P. (2023). Pediatric low-grade glioma: Targeted therapeutics and clinical trials in the molecular era. Neoplasia *36*, 100857. https://doi.org/10.1016/j.neo.2022.100857.

6. Lassaletta, A., Zapotocky, M., Mistry, M., Ramaswamy, V., Honnorat, M., Krishnatry, R., Guerreiro Stucklin, A., Zhukova, N., Arnoldo, A., Ryall, S., et al. (2017). Therapeutic and Prognostic Implications of BRAF V600E in Pediatric Low-Grade Gliomas. J. Clin. Oncol. *35*, 2934–2941. https://doi.org/10.1200/JCO.2016.71.8726.

7. Wang, J., Yao, Z., Jonsson, P., Allen, A.N., Qin, A.C.R., Uddin, S., Dunkel, I.J., Petriccione, M., Manova, K., Haque, S., et al. (2018). A Secondary Mutation in BRAF Confers Resistance to RAF Inhibition in a BRAF(V600E)-Mutant Brain Tumor. Cancer Discov. *8*, 1130–1141. https://doi.org/10.1158/2159-8290.Cd-17-1263.

8. Penman, C.L., Faulkner, C., Lowis, S.P., and Kurian, K.M. (2015). Current Understanding of BRAF Alterations in Diagnosis, Prognosis, and Therapeutic Targeting in Pediatric Low-Grade Gliomas. Front. Oncol. *5*, 54. https://doi.org/10.3389/fonc.2015.00054.

9. Schindler, G., Capper, D., Meyer, J., Janzarik, W., Omran, H., Herold-Mende, C., Schmieder, K., Wesseling, P., Mawrin, C., Hasselblatt, M., et al. (2011). Analysis of BRAF V600E mutation in 1,320 nervous system tumors reveals high mutation frequencies in pleomorphic xanthoastrocytoma, ganglioglioma and extra-cerebellar pilocytic astrocytoma. Acta Neuropathol. *121*, 397–405. https://doi.org/10.1007/s00401-011-0802-6.

10. Shaikh, N., Brahmbhatt, N., Kruser, T.J., Kam, K.L., Appin, C.L., Wadhwani, N., Chandler, J., Kumthekar, P., and Lukas, R.V. (2019). Pleomorphic xanthoastrocytoma: a brief review. CNS Oncol. 8, Cns39. https://doi.org/10.2217/cns-2019-0009.

11. Mistry, M., Zhukova, N., Merico, D., Rakopoulos, P., Krishnatry, R., Shago, M., Stavropoulos, J., Alon, N., Pole, J.D., Ray, P.N., et al. (2015). BRAF mutation and CDKN2A deletion define a clinically distinct subgroup of childhood secondary high-grade glioma. J. Clin. Oncol. 33, 1015–1022. https://doi.org/10.1200/JCO.2014.58.3922.

12. Cantwell-Dorris, E.R., O'Leary, J.J., and Sheils, O.M. (2011). BRAFV600E: implications for carcinogenesis and molecular therapy. Mol. Cancer Ther. 10, 385–394. https://doi.org/10.1158/1535-7163.MCT-10-0799.

13. Krishnatry, R., Zhukova, N., Guerreiro Stucklin, A.S., Pole, J.D., Mistry, M., Fried, I., Ramaswamy, V., Bartels, U., Huang, A., Laperriere, N., et al. (2016). Clinical and treatment factors determining long-term outcomes for adult survivors of childhood low-grade glioma: A population-based study. Cancer 122, 1261–1269. https://doi.org/10.1002/cncr.29907.

14. Huillard, E., Hashizume, R., Phillips, J.J., Griveau, A., Ihrie, R.A., Aoki, Y., Nicolaides, T., Perry, A., Waldman, T., McMahon, M., et al. (2012). Cooperative interactions of BRAFV600E kinase and CDKN2A locus deficiency in pediatric malignant astrocytoma as a basis for rational therapy. Proc. Natl. Acad. Sci. USA 109, 8710–8715. https://doi.org/10.1073/pnas.1117255109.

15. Sievert, A.J., Lang, S.S., Boucher, K.L., Madsen, P.J., Slaunwhite, E., Choudhari, N., Kellet, M., Storm, P.B., and Resnick, A.C. (2013). Paradoxical activation and RAF inhibitor resistance of BRAF protein kinase fusions characterizing pediatric astrocytomas. Proc. Natl. Acad. Sci. USA 110, 5957–5962. https://doi.org/10.1073/pnas.1219232110.

16. de Visser, K.E., and Joyce, J.A. (2023). The evolving tumor microenvironment: From cancer initiation to metastatic outgrowth. Cancer Cell 41, 374–403. https://doi.org/10.1016/j.ccell.2023.02.016.

17. Grabowski, M.M., Sankey, E.W., Ryan, K.J., Chongsathidkiet, P., Lorrey, S.J., Wilkinson, D.S., and Fecci, P.E. (2021). Immune suppression in gliomas. J. Neurooncol. 151, 3–12. https://doi.org/10.1007/s11060-020-03483-y.

18. Bejarano, L., Jordão, M.J.C., and Joyce, J.A. (2021). Therapeutic Targeting of the Tumor Microenvironment. Cancer Discov. 11, 933–959. https://doi.org/10.1158/2159-8290.CD-20-1808.

19. Rajendran, S., Hu, Y., Canella, A., Peterson, C., Gross, A., Cam, M., Nazzaro, M., Haffey, A., Serin-Harmanci, A., Distefano, R., et al. (2023). Single-cell RNA sequencing reveals immunosuppressive myeloid cell diversity during malignant progression in a murine model of glioma. Cell Rep. 42, 112197. https://doi.org/10.1016/j.celrep.2023.112197.

20. Canella, A., Nazzaro, M., Rajendran, S., Schmitt, C., Haffey, A., Nigita, G., Thomas, D., Lyberger, J.M., Behbehani, G.K., Amankulor, N.M., et al. (2023). Genetically modified IL2 bone-marrow-derived myeloid cells reprogram the glioma immunosuppressive tumor microenvironment. Cell Rep. 42, 112891. https://doi.org/10.1016/j.celrep.2023.112891.

21. Griffin, G., Shenoi, S., and Hughes, G.C. (2020). Hemophagocytic lymphohistiocytosis: An update on pathogenesis, diagnosis, and therapy. Best Pract. Res. Clin. Rheumatol. 34, 101515. https://doi.org/10.1016/j.berh.2020.101515.

22. Amankulor, N.M., Kim, Y., Arora, S., Kargl, J., Szulzewsky, F., Hanke, M., Margineantu, D.H., Rao, A., Bolouri, H., Delrow, J., et al. (2017). Mutant IDH1 regulates the tumor-associated immune system in gliomas. Genes Dev. 31, 774–786. https://doi.org/10.1101/gad.294991.116.

23. Nobre, L., Zapotocky, M., Ramaswamy, V., Ryall, S., Bennett, J., Alderete, D., Balaguer Guill, J., Baroni, L., Bartels, U., Bavle, A., et al. (2020). Outcomes of BRAF V600E Pediatric Gliomas Treated With Targeted BRAF Inhibition. JCO Precis. Oncol. 4. https://doi.org/10.1200/PO.19.00298.

24. Xing, Y.L., Panovska, D., and Petritsch, C.K. (2023). Successes and challenges in modeling heterogeneous BRAF(V600E) mutated central nervous system neoplasms. Front. Oncol. 13, 1223199. https://doi.org/10.3389/fonc.2023.1223199.

25. Grossauer, S., Koeck, K., Murphy, N.E., Meyers, I.D., Daynac, M., Truffaux, N., Truong, A.Y., Nicolaides, T.P., McMahon, M., Berger, M.S., et al. (2016). Concurrent MEK targeted therapy prevents MAPK pathway reactivation during BRAFV600E targeted inhibition in a novel syngeneic murine glioma model. Oncotarget 7, 75839–75853. https://doi.org/10.18632/oncotarget.12419.

26. Merritt, C.R., Ong, G.T., Church, S.E., Barker, K., Danaher, P., Geiss, G., Hoang, M., Jung, J., Liang, Y., McKay-Fleisch, J., et al. (2020). Multiplex digital spatial profiling of proteins and RNA in fixed tissue. Nat. Biotechnol. 38, 586–599. https://doi.org/10.1038/s41587-020-0472-9.

27. Becher, B., Schlitzer, A., Chen, J., Mair, F., Sumatoh, H.R., Teng, K.W.W., Low, D., Ruedl, C., Riccardi-Castagnoli, P., Poidinger, M., et al. (2014). High-dimensional analysis of the murine myeloid cell system. Nat. Immunol. 15, 1181–1189. https://doi.org/10.1038/ni.3006.

28. Holland, E.C., Hively, W.P., DePinho, R.A., and Varmus, H.E. (1998). A constitutively active epidermal growth factor receptor cooperates with disruption of G1 cell-cycle arrest pathways to induce glioma-like lesions in mice. Genes Dev. 12, 3675–3685. https://doi.org/10.1101/gad.12.23.3675.

29. Hambardzumyan, D., Amankulor, N.M., Helmy, K.Y., Becher, O.J., and Holland, E.C. (2009). Modeling Adult Gliomas Using RCAS/t-va Technology. Transl. Oncol. 2, 89–95. https://doi.org/10.1593/tlo.09100.

30. Weidenhammer, L.B., Liu, H.Q., Luo, L., Williams, N.T., Deland, K., Kirsch, D.G., and Reitman, Z.J. (2023). Inducing primary brainstem gliomas in genetically engineered mice using RCAS/TVA retroviruses and Cre/loxP recombination. STAR Protoc. 4, 102094. https://doi.org/10.1016/j.xpro.2023.102094.